This is an *Accepted Manuscript*, which has been through the Royal Society of Chemistry peer review process and has been accepted for publication.

Accepted Manuscripts are published online shortly after acceptance, before technical editing, formatting and proof reading. Using this free service, authors can make their results available to the community, in citable form, before we publish the edited article. We will replace this *Accepted Manuscript* with the edited and formatted *Advance Article* as soon as it is available.

You can find more information about *Accepted Manuscripts* in the **Information for Authors**.

Please note that technical editing may introduce minor changes to the text and/or graphics, which may alter content. The journal's standard **Terms & Conditions** and the **Ethical guidelines** still apply. In no event shall the Royal Society of Chemistry be held responsible for any errors or omissions in this *Accepted Manuscript* or any consequences arising from the use of any information it contains.
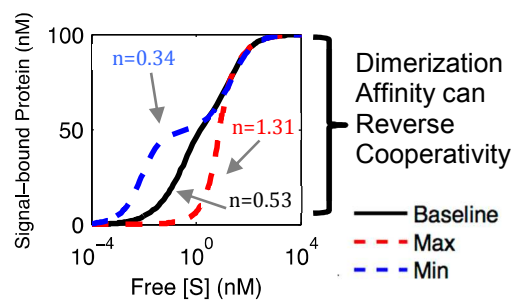
Kinetic modeling reveals that dimerization affinity can increase, eliminate, and even reverse cooperativity imposed by the canonical ligand-affinity mechanism highlighting a novel role for the ubiquitous signaling motif.

Dimerization-based Control of Cooperativity

Mehdi Bouhaddou[1] and Marc R. Birtwistle[1, #]

[1]Icahn School of Medicine at Mount Sinai, Department of Pharmacology and Systems Therapeutics, New York, NY 10029, USA

[#]Corresponding author: marc.birtwistle@mssm.edu

Abstract

Cooperativity of ligand-receptor binding influences the input-output behavior of a biochemical system and thus is an important determinant of its physiological function. Canonically, such cooperativity is understood in terms of ligand-receptor binding affinity, where an initial binding event changes the affinity for subsequent binding events. Here, we demonstrate that dimerization—a simple yet pervasive signaling motif across biology—can have significant control over cooperativity and even dominate over the canonical mechanism. Through an exhaustive parameter sensitivity analysis of a general kinetic model for signal-mediated dimerization, we show that quantitative modulation of dimerization processes can reinforce, eliminate, and even reverse cooperativity imposed by the canonical allosteric ligand-receptor binding affinity mechanism. The favored accumulation of stoichiometrically asymmetric dimers (those with ligand-receptor stoichiometry of 1:2) is a major determinant of dimerization-based cooperativity control. However, simulations demonstrate that favoring accumulation of such stoichiometrically asymmetric dimers can either increase or decrease cooperativity, and thus the quantitative relationship between stoichiometrically asymmetric dimers and cooperativity is highly dependent on the parameter values of the particular system of interest. These results suggest that the dimerization motif provides a novel mechanism for both generating and quantitatively tuning cooperativity that, due to the ubiquity of dimerization motifs in biochemical systems, may play a major role in a host of biological functions. Thus, the canonical, allosteric view of cooperativity is incomplete without considering dimerization effects, which is of particular importance as dimerization is often a necessary feature of the allosteric mechanism.

Introduction

Protein dimerization is ubiquitous in nature and is essential to numerous cellular and physiological functions. It is estimated that approximately two-thirds of known proteins form dimers or higher-order oligomers[1], and that the dimer interface of many dimerizing proteins is more highly conserved than the rest of the protein surface[2], highlighting the importance of dimerization in numerous biochemical systems. In general, dimerization can endow proteins and biochemical systems with important advantages, such as increased stability, specificity, and complexity[3]. For instance, dimerization can induce the formation of an active site that is not present in the singular monomer, which has been observed for numerous caspases, such as Caspase 9[4]. Combinatorial specificity can be achieved when monomers can mix-and-match to generate a unique signal from each combination; for example, the *E. coli* protein BirA can act either as an essential metabolic enzyme or a transcriptional repressor, depending on the adaptor molecules to which it is bound[5]. In addition, dimerization can mediate allosteric regulation between binding sites by facilitating conformational changes (e.g. oxygen-hemoglobin[6-12]), leading to highly cooperative binding.

In many systems, the binding of a "signal" (an activated protein, peptide ligand, hormone, metabolite, etc.), which we call "S", influences dimerization of its protein target, which we call "P", and this dimerization event facilitates a downstream response. For instance, in many cases when a ligand binds its cognate receptor tyrosine kinase, it induces receptor dimerization, which affects downstream signaling[13]. This mechanism is not only limited to extracellular ligand/cell surface receptor systems, but can also apply to intracellular signaling cascades. For example, when active GTP-bound Ras binds Raf kinase it promotes Raf dimerization, which is required for wild-type Raf activity[14]. In addition, principally in bacteria and other prokaryotes, DNA induces the dimerization of type II restriction enzymes (e.g. BamH1), switching on their enzymatic activity[15].

One important feature of any signaling system is the quantitative nature of its steady-state, input-output response. This is often described in terms of cooperativity or ultrasensitivity and is quantified by a Hill coefficient, which indicates the effective cooperativity behavior. For example, the phosphorylation of cdc25C by cdk1, which is a critical step driving the cell cycle transition from G2 into mitosis, was shown to ensue with positive cooperativity and a Hill coefficient greater than one[16], resulting in a strong and immediate all-or-none transition into mitosis to avoid the potentially lethal consequences of an uncoordinated transition. Conversely, EGF binding to EGFR ensues with negative cooperativity and a Hill coefficient less than one[17], which would allow the EGFR system to respond more gradually to a wider range of growth factor concentrations[18].

Effective cooperativity is currently understood to be controlled either (*i*) at the initial level of a signal (e.g. ligand) binding to its downstream protein (e.g. receptor), where allosteric interactions cause the initial signal binding event to increase or decrease affinity for subsequent binding events, or (*ii*) by systems-level effects, such as explicit positive or negative feedback or multi-tiered cascades[19-22]. Here, we show how dimerization processes by themselves can control effective cooperativity in a manner that dominates over the first mechanism, revealing both a novel role for the widespread dimerization motif and a new Hill coefficient tuning mechanism. Although many studies

have investigated cooperativity in dimerizing systems, their focus is largely on the effects of ligand- ("signal-" in our model) binding affinity, or another mechanism specific to their system, as the driver of cooperativity[23-28]. The notion that dimerization alters dose-response properties of a biochemical system has been mentioned by a few prior studies[29-33], but the extent to which it can alter cooperativity has not been explicitly investigated in a general sense. Most importantly, none have investigated how changes in dimerization affinity can reverse canonical, ligand affinity-induced cooperativity from being negative to positive and vice versa. Through an exhaustive parameter sensitivity analysis of a general kinetic model for signal-mediated dimerization, we show that dimerization processes can increase, eliminate, and even reverse signal binding-induced cooperativity. Simulations suggest that this dimerization-based control of cooperativity is largely mediated by the favored accumulation of stoichiometrically asymmetric dimers (i.e. dimers with a signal-to-target protein ratio of 1:2) which sequester signal binding sites, consistent with previous work[29-33]. Further analyses reveal that changes in dimerization affinity leading to the accumulation of such stoichiometrically asymmetric dimers can increase or decrease cooperativity, and that the quantitative relationship between stoichiometrically asymmetric dimers and cooperativity depends largely on how key signal-binding parameters are configured. Our findings demonstrate that the canonical, allosteric view of cooperativity is incomplete without considering dimerization effects. This is of particular importance as dimerization is often a necessary feature of the allosteric mechanism. In addition to the aforementioned ideas, the widespread presence of dimerization motifs in biology may be related to their ability to tune cooperativity both in a coarse and fine sense, thus influencing phenotypes through quantitative properties of input-output responses.

Results and Discussion

Different Dimerization Schemes Cause Widely Varying Cooperativity Behavior

To begin exploring how the dimerization motif affects cooperativity and ultrasensitivity, we consider the situation where a signal, S, binds to a downstream protein, P, and the downstream protein dimerizes (Fig. 1A). This could represent a host of biological systems as described above. To analyze dose-response curves and their resulting cooperativity/ultrasensitivity behavior, we compute Hill coefficients based on both traditional Scatchard analysis ("Scatchard n—n_s"—indicator of cooperativity) and a more biologically relevant "functional" analysis ("Functional n—n_f"—indicator of ultrasensitivity). Scatchard dose-response curves are calculated by summing all signal-bound species on the y-axis ([SP]+[SPP]+2*[SPSP]) whereas functional dose-response curves are calculated by summing only the signal-induced biologically active dimer species on the y-axis ([SPP]+[SPSP]). Both are plotted against free [S] (unbound S) on the x-axis. A Hill coefficient $n=1$ indicates the absence of effective cooperativity/ultrasensitivity, an $n<1$ indicates effective negative cooperativity/ultrasensitivity, and an $n>1$ indicates effective positive cooperativity/ultrasensitivity. We also present the traditional Scatchard plots (Fig. 1, right panels), which give a qualitative indication of cooperativity[34, 35]. A linear Scatchard plot indicates the absence of cooperativity, a concave-up plot indicates negative cooperativity,

and a concave-down plot indicates positive cooperativity. For simplicity, from here on we refer only to the term cooperativity rather than both cooperativity and ultrasensitivity.

When all rate constants in the entire scheme are set to unity, there is no effective cooperativity (Fig. 1A). To illustrate how extreme dimerization variant cases of this scheme can alter this base cooperativity behavior we consider two scenarios. First, when S binds P and then SP dimerizes with an additional downstream protein, P, the stoichiometrically asymmetric dimer, SPP, results and the cooperativity is negative, indicated by Hill coefficients less than one and a concave-up Scatchard plot (Fig. 1B). This systems-level negative cooperativity arises from the fact that binding sites are sequestered in the stoichiometrically asymmetric dimer, SPP. The functional analysis (Fig. 1B, middle, green dashed line) displays non-monotonicity here because at high [S], all of the P is contained in SP molecules, precluding formation of SPP. When S binding P is followed by the dimerization between two SP molecules, positive cooperativity results as indicated by Hill coefficients greater than one and a concave-down Scatchard plot; the functional analysis shows a similar trend (Fig. 1C). This model could represent estrogen receptor signaling, where the dimerization of two hormone-bound receptors stimulates DNA binding and transcriptional activation[36]. Accordingly, estrogen receptor signaling has been reported to display positive cooperativity[37]. Notably, this scheme is often the one assumed in models of RTK signaling,[38-41] despite the fact many RTKs exhibit negative cooperativity.

Dimerization Can Reverse Canonical Negative or Positive Cooperativity

We hypothesized that since inclusion of different dimerization mechanisms alters system cooperativity, changes in dimerization rate constant parameters could control cooperativity in this system. We further thought that dimerization processes may even be able to reverse negative or positive cooperativity caused by the canonical allosteric mechanism, where the signal explicitly has a different affinity for the second binding event.

To test this hypothesis, we explored the range of Hill coefficients obtainable by only altering dimerization rate constant parameters (those belonging to reaction rates v_3, v_4, v_5, v_6, v_{11}, and v_{12}) while keeping signal binding rate constant parameters fixed (those belonging to reaction rates v_1, v_2, v_7, v_8, v_9, and v_{10}), similar to a parameter variation study of MAPK signaling dynamics[42]. This is done to show the extent to which the modulation of dimerization rate constants can alter cooperativity. To perform this parameter sensitivity analysis, we allowed all rate constant parameters to take one of three possible values—0.1, 1, or 10 (s^{-1} or $s^{-1}nM^{-1}$)—and then calculated n_s and n_f (Fig. 2). Each horizontal bar corresponds to a single, fixed set of signal binding rate constants while all possible sets of dimerization rate constants are explored and the resulting range of Hill coefficients is recorded (see Fig. 2A for graphical description). Thus, there are 3^6 horizontal bars, one for each possible set of signal binding rate constants (3 possible values for each of 6 rate constant parameters), where each bar is populated by 3^6 simulation-derived Hill coefficients (one for each possible set of dimerization rate constant parameters). The central dark blue sections of each bar denote Hill coefficients between the 5th and 95th percentiles and the light blue tips span the remaining 5% on either side. The red dots on each bar signify the Hill coefficient when all dimerization rate constants are set to unity for that particular set of signal binding rate constants,

representing a "baseline" for each set of signal binding rate constants before dimerization rate constants are modulated.

As the data depict, changes in dimerization rate constants can strongly alter Hill coefficients independently of changes in signal binding rate constants. For systems that naturally have negative cooperativity (red dot left of the black dashed line) or positive cooperativity (red dot right of the black dashed line) dimerization rate constant changes can (*i*) reinforce cooperativity (*n*>1 becoming larger or *n*<1 becoming smaller), (*ii*) eliminate cooperativity (*n* approaches 1) or, (*iii*) reverse cooperativity (*n*>1 becoming *n*<1 or vice versa). Thus, dimerization can actually dominate over the canonical allosteric mechanism for generating cooperativity. These results hold true regardless of whether a Scatchard or functional analysis is used (compare Fig. 2B to 2C). Interestingly, in the Scatchard case, when all signal binding k_{on} rates are equal and all signal binding k_{off} rates are equal (e.g. when $k_2, k_8, k_{10}=10$ and $k_1, k_7, k_9=0.1$) and baseline cooperativity is thus absent (*n*=1), changes in dimerization affinity are not able to alter the cooperativity of the system (there are nine occurrences of this in our data set). This suggests, in the case of Scatchard-based analysis, that some cooperativity must be pre-imposed by signal-binding parameters in order for dimerization to be able to affect cooperativity. This result did not hold for the functional Hill coefficient analysis, however.

In order to determine whether our results applied to other signal-induced dimerization mechanisms, we ran the same analysis on two additional models that depicted interactions between (*1*) a bivalent-ligand and a homodimer receptor (Fig. S1B-C) or (*2*) a bivalent-ligand and heterodimer receptors (Fig. S1D-E). We indeed found that changes in dimerization parameters can also reinforce, eliminate, and reverse cooperativity imposed by the canonical allosteric mechanism, just as in the general kinetic scheme (above).

The parameter sets used for our simulations do not satisfy detailed balance. Detailed balance assumptions hold when there are no changes in free energy along a cycle. From a biological perspective, detailed balance is quite restrictive, since signal-induced dimerization events are often linked to energy-generating mechanisms, such as ATP hydrolysis, even if not explicitly modeled. Thus, detailed balance equations may be inconsistent with many relevant biological situations of interest in our study. Nevertheless, we generated parameter sets that satisfied detailed balance to test whether our main conclusions hold. We find that dimerization affinity can still alter cooperativity and even reverse it for both the Scatchard and functional case (Fig. S2B and S2C), although for very strong base positive cooperativity, it may not be possible to reverse but rather only modulate cooperativity.

What do the dose response curves look like when dimerization causes a reversal of canonical cooperativity? Figure 3 shows specific examples of how dimerization affinity can reverse or reinforce cooperativity for three different sets of signal-binding parameters: one that intrinsically yields negative cooperativity (Fig. 3A), positive cooperativity (Fig. 3B), or no cooperativity (Fig. 3C). For instance, at baseline, the simulation depicted in Figure 3A (left) produces a dose-response curve that possesses negative cooperativity (n_s=0.53; solid black line). Changes in dimerization rate constants alone can both profoundly reduce (n_s=0.34; blue dashed line) or increase (n_s=1.31; red dashed line) the cooperativity of the curve, even though signal-binding rate constants are unchanged. Similar results are obtained for the functional analysis, run using the same

signal-binding parameters (Fig. 3A, right), and the remainder of cases as well (Fig. 3B-C).

Taken together, these results suggest that hard-wired dimerization affinity likely plays a significant role in determining the cooperativity behavior of numerous biochemical systems. In addition, biochemical systems could regulate dimerization affinity in order to fine-tune and/or completely alter their cooperativity behavior. For example, from a biological perspective, one function of ligand-less receptors that act as obligate dimerization partners, such as ErbB2 or p75 neurotrophin receptor, may be to tune cooperativity through their expression levels[43, 44]. From a pharmacological perspective, drugs that act by inhibiting dimerization, such as trastuzumab or pertuzumab (for ErbB2 positive breast cancer[45]), may not only inhibit signaling directly, but may also alter the cooperativity and dose response of the system. Understanding this may lend novel insight into how drugs of this kind mediate their therapeutic or toxic effects.

Stoichiometrically Asymmetric Dimer Behavior is a Major Determinant of Cooperativity

How does dimerization control cooperativity? Previous work has suggested that the stoichiometrically asymmetric dimer, SPP, plays a central role [29-33]. Based on this, we hypothesized that the SPP molecule would be more abundant in simulations with low Hill coefficients and vice-versa. Using the data generated by the exhaustive parameter sensitivity analysis described above (a total of $3^{12} = 531,441$ simulations), we plotted the Hill coefficient versus the integral of steady-state [SPP] over a range of initial signal concentrations ($[S]_0$). We termed this quantity "SPP area" (see Fig. 4A for graphical description). SPP area has a significant negative correlation with both the Scatchard ($\rho=-0.48$, $p<0.001$; Fig. 4B) and functional ($\rho=-0.23$, $p<0.001$; Fig. 4C) Hill coefficients. The relationship appears to exhibit a $1/x$-type dependence, meaning that positive cooperativity only seems to be possible when SPP area is low. The same analysis done with the parameter sets that satisfy detailed balance gave highly similar results (Fig. S3).

Our reasoning for why the accumulation of SPP drives negative cooperativity is that SPP sequesters two downstream P molecules for every signal S molecule, disrupting the stoichiometric balance between S and P. In other words, each time an SPP molecule is formed, a potential binding site for an S molecule is removed. This imbalance leads to an increased ratio of free [S] to free [P], which is a hallmark of negative cooperativity as defined by Scatchard analysis. Conversely, a decrease in the ratio of free [S] to free [P] is an indicator of positive cooperativity. Thus, it appears that dimerization controls cooperativity by hijacking the canonical allosteric mechanism.

How Stoichiometrically Asymmetric Dimers Affect Cooperativity is Highly Parameter Dependent

The overall negative correlation between SPP area and cooperativity (Fig. 4B) implies that if one favors accumulation of SPP, then the system should be more negatively cooperative. We wondered whether this trend was general, or if there might be a different dependence of cooperativity on SPP area for specific sets of signal-binding parameters (which correspond to individual bars in Fig. 2B). To explore this, we looked at changes in SPP area while altering dimerization parameters but keeping signal-binding parameters constant, and calculated a Pearson's r correlation coefficient between SPP

area and Scatchard hill coefficients across each set of fixed signal-binding parameters. Surprisingly, we found that many parameter sets' cooperativity behavior is positively correlated with SPP area (Figure 5A, top vs. bottom panel), opposite to the general trend. We found this correlation behavior to depend heavily on the baseline Hill coefficient for each set (Figure 5B; $p<10^{-102}$); systems that inherently display negative cooperativity show a negative correlation (similar to the general trend), while systems that inherently display positive cooperativity show a positive correlation. Mechanistically, this correlation seems to be controlled by a ratio between the dissociation constants (K_d) of the signal binding reactions surrounding SPP in our scheme ($K_{d9,10} / K_{d7,8}$) (Fig. 5C). When this ratio is small, increased SPP area leads to increased cooperativity, but when this ratio is large, increased SPP area leads to decreased cooperativity.

Based on this logic, a particular system's dimerization parameters could be theoretically configured to favor or disfavor SPP accumulation, and thus tune the resulting Hill coefficient. However, the tuning direction depends on how signal binding parameters are configured. Thus, although accumulation of SPP was previously considered to be the main determinant of cooperativity, this analysis shows that how SPP controls cooperativity is highly dependent on the particular parameters of the whole system, namely, the baseline signal-binding cooperativity behavior. Thus, generally favoring SPP abundance will not always result in a more negatively cooperative system.

Conclusions

We show that dimerization processes can significantly alter the cooperativity behavior of a system and can even reverse the canonical, allosteric mechanism of negative or positive cooperativity. These findings indicate that the canonical allosteric view of cooperativity is incomplete without considering dimerization effects; this is particularly important because dimerization is often a necessary feature of the allosteric mechanism. Furthermore, these findings suggest that one reason for the widespread presence of dimerization motifs in biology may be to tune and/or reverse the cooperativity behavior of biochemical systems—a function that is likely critical to the proper functioning of various signaling systems. We suggest that this cooperativity-altering function of dimerization is largely driven by the accumulation of stoichiometrically asymmetric dimer species. However, the effect of stoichiometrically asymmetric dimer accumulation on the Hill coefficient is dependent on the baseline signal binding parameters.

Gaining a more in-depth understanding of the relationships between dimerization and cooperativity in disease may lead to a more rational drug-design process, whereby certain dimer species could be preferentially targeted over others. In addition, this understanding may help us better understand how current drugs that alter dimerization function may have otherwise overlooked affects on systems-level behaviors such as tuning input-output responses through cooperativity.

Methods

Model Simulation

Chemical kinetics theory with mass action kinetics was used to derive a differential equation model for each scheme in the manuscript (see Supplementary Information for equations). Models were simulated to steady-state using MATLAB (The Mathworks, Natick, MA) with the function `ode15s`.

Dose Response Curves and Scatchard Analysis

For each simulation, 25 log-spaced values for initial signal concentrations, $[S]_0$, were explored, ranging from 10^{-2} to 10^3 nM. Each simulation began with an initial downstream target protein concentration, $[P]_0$, of 100 nM. Steady-state values for each species, at each designated $[S]_0$, were used to generate a dose-response curve. Dose-response curves were generated by plotting free $[S]$ versus the sum of signal-bound species ($[SP] + [SPP] + 2*[SPSP]$) for Scatchard analysis and the sum of signal-induced biologically active dimers ($[SPP] + [SPSP]$) for the functional analysis. The Hill coefficients were calculated by fitting the Hill equation to the simulated data using a least squares method with the MATLAB function `lsqcurvefit`. This Hill equation is given by:

$$Y = \frac{Y_{max}[S]^n}{K_{50}^n + [S]^n} \tag{1}$$

where Y is the output (sum of signal bound species), Y_{max} is the maximum level of Y, *[S]* is free signal concentration, K_{50} is the *[S]* at which $Y=Y_{max}/2$, and n is the Hill coefficient. For the functional analysis, Hill coefficients were determined using only the portion of the curve prior to the maximum to avoid potentially erroneous calculations due to non-monotonicity (see Fig. S4 for an example fit). Dose response curves and Scatchard plots in Figure 1 were generated with all kinetic parameters set to unity.

Exhaustive Parameter Sensitivity Analysis

Each of the twelve rate constants in the complete model (Fig. 1A) was allowed to take one of three possible values: 0.1, 1, or 10 (s^{-1} or $s^{-1}nM^{-1}$). Every possible permutation of the parameters was simulated, resulting in 3^{12} (or 531,441) different parameter sets. For each parameter set, dose response curves were generated and Hill coefficients estimated as described above. Only simulations that can satisfy the following equations (depicting the two major cycles: R+L→LR+R→LRR→L+RR→R+R and LR+LR→LRLR→L+LRR→R+LR→L+R) are able to satisfy detailed balance:

$$\frac{k2}{k1} \cdot \frac{k6}{k5} \cdot \frac{k7}{2 \cdot k8} \cdot \frac{k3}{k4} = 1 \tag{2}$$

$$\frac{k12}{k11} \cdot \frac{2 \cdot k9}{k10} \cdot \frac{k5}{k6} \cdot \frac{k2}{k1} = 1 \tag{3}$$

Thus, none of our parameter sets satisfied detailed balance as they were. We generated parameter sets that satisfied detailed balance by solving for k_4 and k_{12} such that Eq. 2 and Eq. 3 were satisfied, while keeping all other rate constants as they were for each of the 3^{12} simulations. We used this data in Figures S2 and S3.

Calculating area under the SPP curve ("SPP area")
To calculate the area under the SPP dose-response curve, [SPP] steady-state values were plotted versus $[S]_0$ and the integral under the curve was calculated for each simulation using the MATLAB function `trapz`. The example in Figure 4A was computed with the following rate constants: $k_1,k_2,k_6,k_7,k_8,k_9,k_{10}=1$, $k_3,k_{11}=10$, and $k_4,k_5,k_{12}=0.1$. Area values were plotted versus the Hill coefficients for all 3^{12} simulations.

Examples of SPP area and boxplots in Figure 5
Example sets in Figure 5A possessed the following signal-binding rate constants from left-to-right: $k_1,k_2,k_7,k_8,k_9,k_{10}$=[0.1,1,10,0.1,0.1,10], [0.1,1,0.1,1,0.1,10], [1,0.1,10,0.1,1,0.1], [1,0.1,10,0.1,1,1], [10,0.1,1,1,0.1,0.1], [0.1,0.1,0.1,10,0.1,0.1], [10,0.1,0.1,10,1,1], [10,1,1,1,10,0.1]. For the boxplots, the central red line is the median, the edges of the box are the 25th and 75th percentiles, and the whiskers extend to the maximum and minimum values not considered outliers. Points are defined as outliers if they are greater than *q3+w(q3-q1)* or smaller than *q1-w(q3-q1)*, where *w*=1.5.

Acknowledgements

Author Contributions
MB and MRB conceived of the study, designed and performed the analyses as well as wrote and edited the manuscript.

References

1.   J. M. Matthews and M. Sunde, in *Protein dimerization and oligomerization in biology*, ed. J. M. Matthews, Landes Bioscience and Springer Science+Business Media, 2012, ch. 1, pp. 1-18.
2.   S. Dey, A. Pal, P. Chakrabarti and J. Janin, *Journal of molecular biology*, 2010, 398, 146-160.
3.   N. J. Marianayagam, M. Sunde and J. M. Matthews, *Trends in biochemical sciences*, 2004, 29, 618-625.
4.   M. Renatus, H. R. Stennicke, F. L. Scott, R. C. Liddington and G. S. Salvesen, *Proceedings of the National Academy of Sciences of the United States of America*, 2001, 98, 14250-14255.
5.   J. E. J. Cronan, *Cell*, 1989, 58, 427-429.
6.   G. S. Adair, *The Journal of biological chemistry*, 1925, 63, 529-545.
7.   A. F. Riggs, *Journal of Experimental Biology*, 1998, 201, 1073-1084.

8.   Y. Qiu, D. H. Maillett, J. Knapp, J. S. Olson and A. F. Riggs, *Journal of Biological Chemistry*, 2000, 275, 13517-13528.
9.   H. A. Heaslet and W. E. Royer, Jr., *The Journal of biological chemistry*, 2001, 276, 26230-26236.
10.   J. Wyman, 1948, 4, 407-531.
11.   J. Wyman and D. W. Allen, *Journal of Polymer Science*, 1951, 7, 499-518.
12.   J. Monod, J. Wyman and J. Changeux, *Journal of molecular biology*, 1965, 12, 88-118.
13.   A. Ullrich and J. Schlessinger, *Cell*, 1990, 61, 203-212.
14.   L. K. Rushworth, A. D. Hindley, E. O'Neill and W. Kolch, *Molecular and cellular biology*, 2006, 26, 2262-2272.
15.   A. Pingoud and A. Jeltsch, *Nucleic Acids Res*, 2001, 29, 3705-3727.
16.   N. B. Trunnell, A. C. Poon, S. Y. Kim and J. E. Ferrell, Jr., *Molecular cell*, 2011, 41, 263-274.
17.   D. Alvarado, D. E. Klein and M. A. Lemmon, *Cell*, 2010, 142, 568-579.
18.   M. R. Birtwistle and W. Kolch, *Cell cycle*, 2011, 10, 2069-2076.
19.   B. N. Kholodenko, J. B. Hoek, H. V. Westerhoff and G. C. Brown, *FEBS Letters*, 1997, 414, 430-434.
20.   C. F. Huang and J. E. Ferrell, Jr., *Proceedings of the National Academy of Sciences of the United States of America*, 1996, 93, 10078-10083.
21.   N. Blüthgen and H. Herzel, *Journal of theoretical biology*, 2003, 225, 293-300.
22.   N. Blüthgen, S. Legewie, H. Herzel and B. N. Kholodenko, in *Introduction to Systems Biology*, Humana Press, 2007, pp. 282-299.
23.   D. Barua, J. R. Faeder and J. M. Haugh, *Plos Computational Biology*, 2009, 5, 1-9.
24.   D. Barua, J. R. Faeder and J. M. Haugh, *The Journal of biological chemistry*, 2008, 283, 7338-7345.
25.   H. Kaur, C. S. Park, J. M. Lewis and J. M. Haugh, *The Biochemical journal*, 2006, 393, 235-243.
26.   J. M. Haugh, *Biotechnology Progress*, 2004.
27.   R. G. Posner, B. Lee, D. H. Conrad, D. Holowka, B. Baird and B. Goldstein, *Biochemistry*, 1992, 31, 5350-5356.
28.   F. Mac Gabhann and A. S. Popel, *Biophysical chemistry*, 2007, 128, 125-139.
29.   A. Levitzki and J. Schlessinger, *Biochemistry*, 1974, 13, 5214-5219.
30.   G. K. j. Wolfer, J. L. j. Neil and W. B. Rippon, *J Protein Chem*, 1987, 6, 441-454.
31.   S. G. Chamberlin and D. E. Davies, *Biochim Biophys Acta*, 1998, 1384, 223-232.
32.   M. A. Lemmon, *Experimental cell research*, 2009, 315, 638-648.
33.   J. L. Macdonald and L. J. Pike, *Proceedings of the National Academy of Sciences of the United States of America*, 2008, 105, 112-117.
34.   G. Scatchard, *Ann N Y Acad Sci*, 1949, 51, 660-672.
35.   C. Wofsy, B. Goldstein, K. Lund and S. H. Wiley, *Biophysical journal*, 1992, 63, 98-110.
36.   H. Wang, G. A. Peters, X. Zeng, M. Tang, W. Ip and S. A. Khan, *The Journal of biological chemistry*, 1995, 270, 23322-23329.
37.   A. C. Notides, N. Lerner and D. E. Hamilton, *Proceedings of the National Academy of Sciences of the United States of America*, 1981, 78, 4926-4930.

38. B. N. Kholodenko, O. V. Demin, G. Moehren and J. B. Hoek, *Journal of Biological Chemistry*, 1999, 274, 30169-30181.
39. M. R. Birtwistle, M. Hatakeyama, N. Yumoto, B. A. Ogunnaike, J. B. Hoek and B. N. Kholodenko, *Molecular systems biology*, 2007, 3, 144.
40. B. Schoeberl, C. Eichler-Jonsson, E. D. Gilles and G. Muller, *Nat Biotechnol*, 2002, 20, 370-375.
41. W. W. Chen, B. Schoeberl, P. J. Jasper, M. Niepel, U. B. Nielsen, D. A. Lauffenburger and P. K. Sorger, *Molecular systems biology*, 2009, 5, 239.
42. L. Qiao, R. B. Nachbar, I. G. Kevrekidis and S. Y. Shvartsman, *PLoS Computational Biology*, 2007, 3, 1819-1826.
43. Y. Li, J. Macdonald-Obermann, C. Westfall, D. Piwnica-Worms and L. J. Pike, *The Journal of biological chemistry*, 2012, 287, 31116-31125.
44. M. V. Chao, *Nature reviews. Neuroscience*, 2003, 4, 299-309.
45. M. C. Franklin, K. D. Carey, F. F. Vajdos, D. J. Leahy, A. M. de Vos and M. X. Sliwkowski, *Cell*, 2004, 5, 317-328.
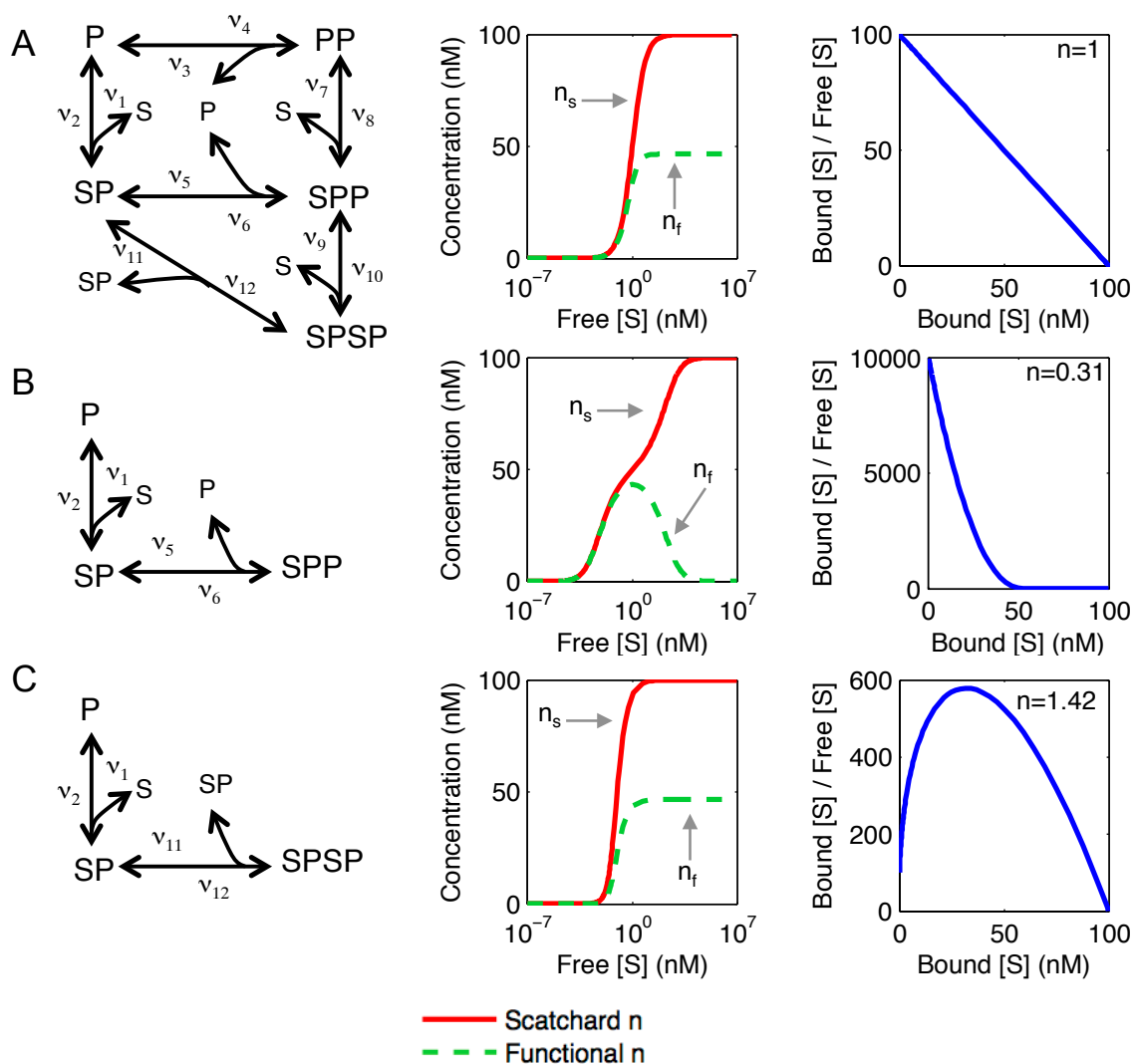
Figure 1. The cooperativity behavior resulting from different dimerization schemes.
Figure 1 depicts a kinetic scheme, dose-response curves, and a Scatchard plot (left-to-right, respectively) for the full model and various model subsets when all rate constant parameters are set to unity. (A) Complete model schematic depicting all possible species resulting from the binding and dimerization interactions between a signal, S, a downstream protein, P, and the complex SP. This results in no cooperativity. (B) A schematic of S binding P, followed by the dimerization of SP with an additional P, resulting in the stoichiometrically asymmetric dimer, SPP. This results in negative cooperativity. (C) A schematic of S binding P, followed by the dimerization between two SP molecules, resulting in the stoichiometrically symmetric dimer, SPSP. This results in positive cooperativity.
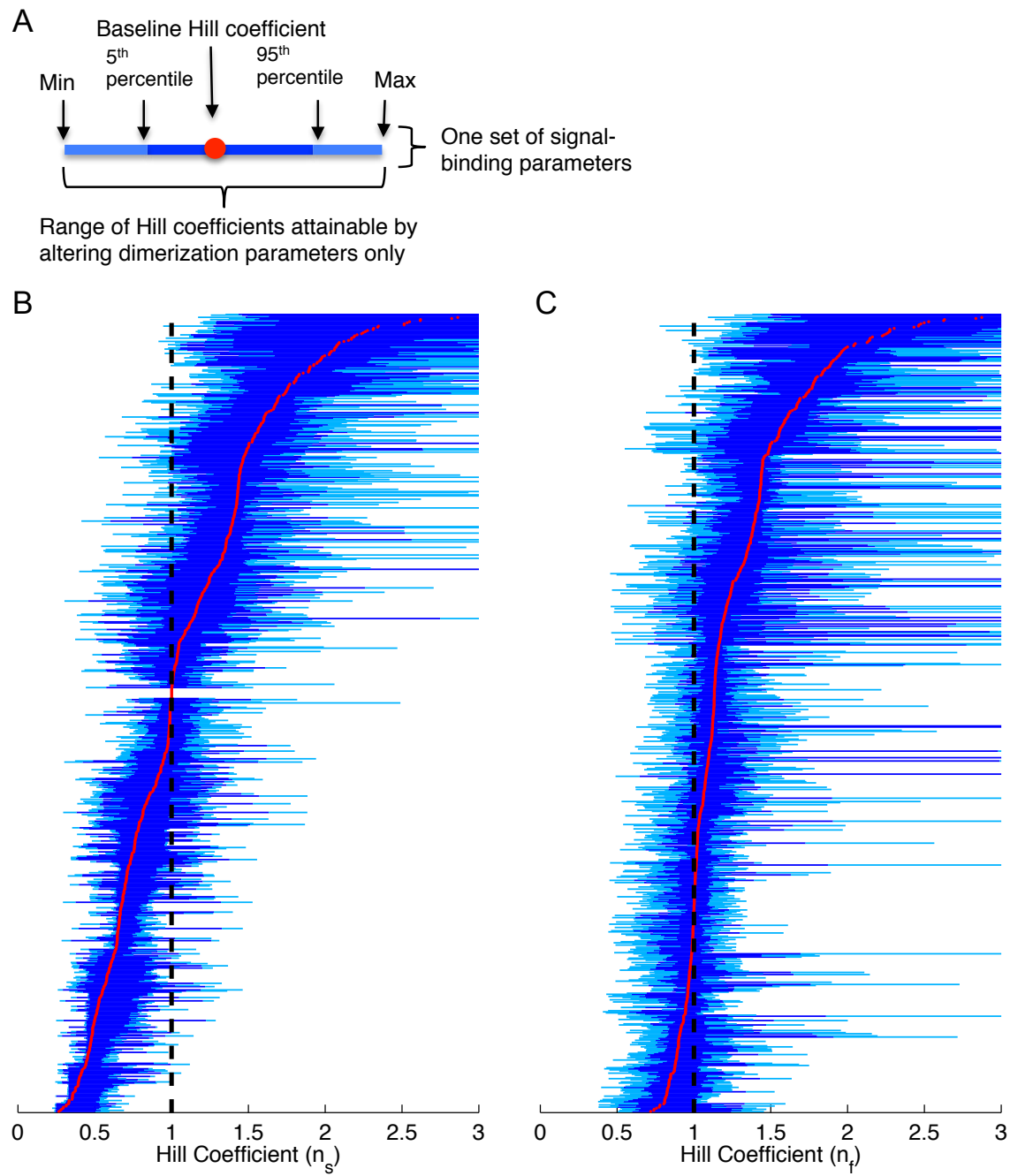
Figure 2. The effect of dimerization affinity on cooperativity behavior.
(A) Graphical description of each horizontal bar (in B and C). Each horizontal bar corresponds to 729 (3^6) simulations and spans the range of Hill coefficients attainable by altering dimerization rate constants while keeping signal-binding rate constants fixed. The dark blue section of each bar denotes Hill coefficients between the 5th and 95th percentiles and the light blue tips span the remaining 5% on either side. Each bar contains a single red dot, indicating the "baseline" Hill coefficient when all dimerization rate constants are set to unity. (B) Results for Scatchard Hill coefficients (n_s). (C) Results for functional Hill coefficients (n_f). In B and C, the dashed line divides negative cooperativity values on the left ($n<1$) from positive cooperativity values on the right ($n>1$).
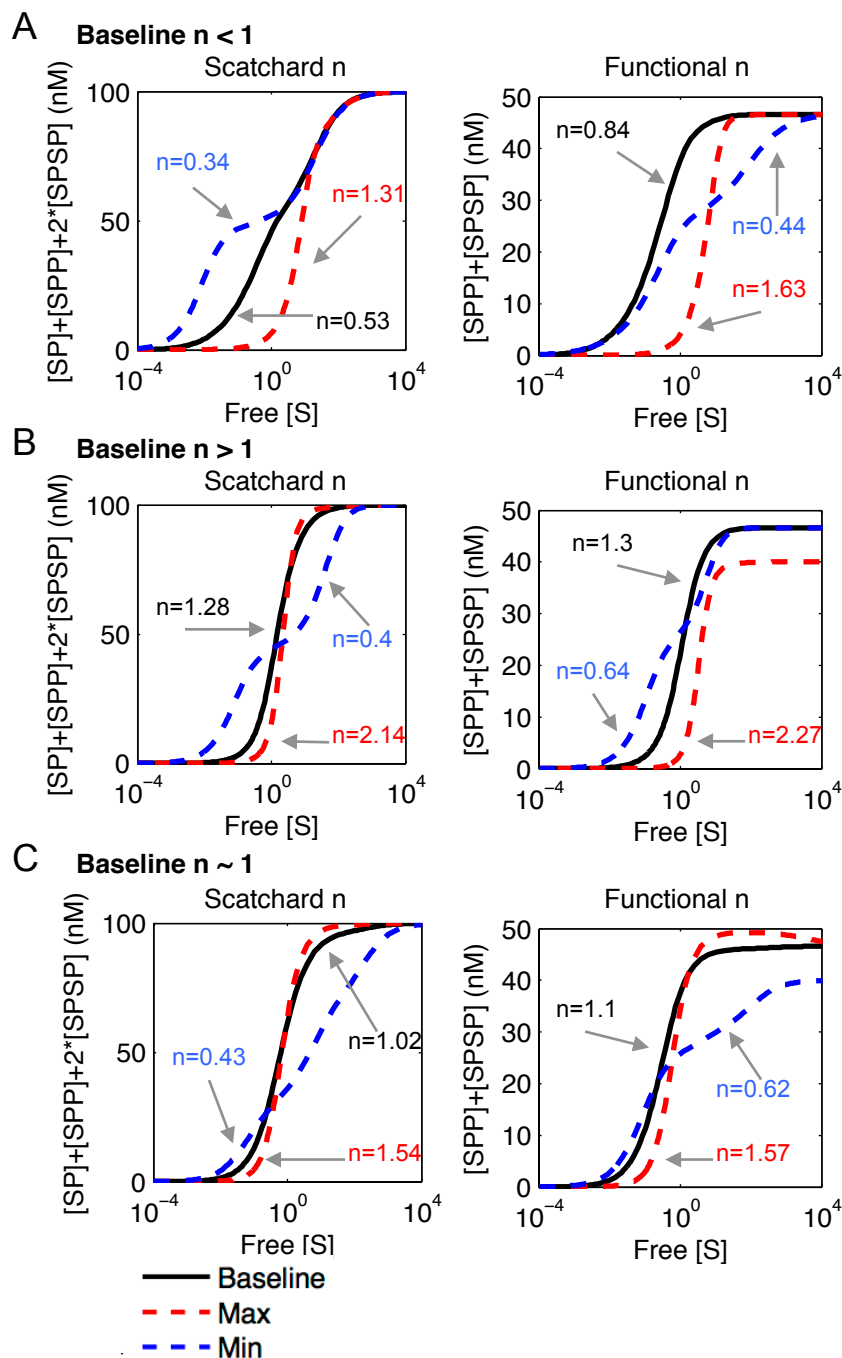
Figure 3. Examples of dimerization rate constants reversing and reinforcing cooperativity behavior. In all Panels, dimerization rate constants are modulated and signal-binding rate constants are held constant. The Scatchard analyses are on the left and the functional analyses are on the right. Solid black lines refer to the baseline case, when all dimerization parameters are set to unity, the red and blue dashed lines denote the dose-response curves possessing the maximum and minimum hill coefficients, respectively, induced by changing dimerization rate constants. (A) Example simulation when the baseline $n<1$. The signal-binding rate constants are: $k_1, k_7, k_8 = 0.1$, $k_{10} = 1$, and $k_2, k_9 = 10$. The dose-response curves for max Scatchard ($k_3, k_6, k_{11} = 0.1$, $k_4, k_5, k_{12} = 10$), min Scatchard ($k_4, k_5, k_{11} = 0.1$, $k_3, k_6, k_{12} = 10$), max functional ($k_3, k_6 = 0.1$, $k_4, k_5, k_{11}, k_{12} = 10$), and min functional ($k_4, k_6, k_{11}, k_{12} = 0.1$, $k_3, k_5 = 10$) are displayed alongside their respective hill coefficients. (B) Example simulation when the baseline $n>1$. The signal-binding rate constants are:

$k_8,k_9,k_{10}=0.1$, $k_7=1$, and $k_1,k_2=10$. The dose-response curves for max Scatchard ($k_3,k_6,k_{11},k_{12}=0.1$, $k_4=1$, $k_5=10$), min Scatchard ($k_4,k_5,k_{12}=0.1$, $k_3,k_6,k_{11}=10$), max functional ($k_3,k_6=0.1$, $k_4,k_{12}=1$, $k_5,k_{11}=10$), and min functional ($k_4,k_5=0.1$, $k_3=1$, $k_6,k_{11},k_{12}=10$) are displayed alongside their respective hill coefficients. (C) Example simulation when the baseline $n\sim1$. The signal-binding rate constants are: $k_2,k_7,k_9=0.1$, $k_8,k_{10}=1$, and $k_1=10$. The dose-response curves for max Scatchard ($k_3,k_{11},k_{12}=0.1$, $k_4,k_5,k_6=10$), min Scatchard ($k_3,k_4,k_5,k_6,k_{12}=0.1$, $k_{11}=10$), max functional ($k_3,k_{11},k_{12}=0.1$, $k_4,k_5,k_6=10$), and min functional ($k_4,k_5,k_6=0.1$, $k_{12}=1$, $k_3,k_{11}=10$) are displayed alongside their respective hill coefficients.
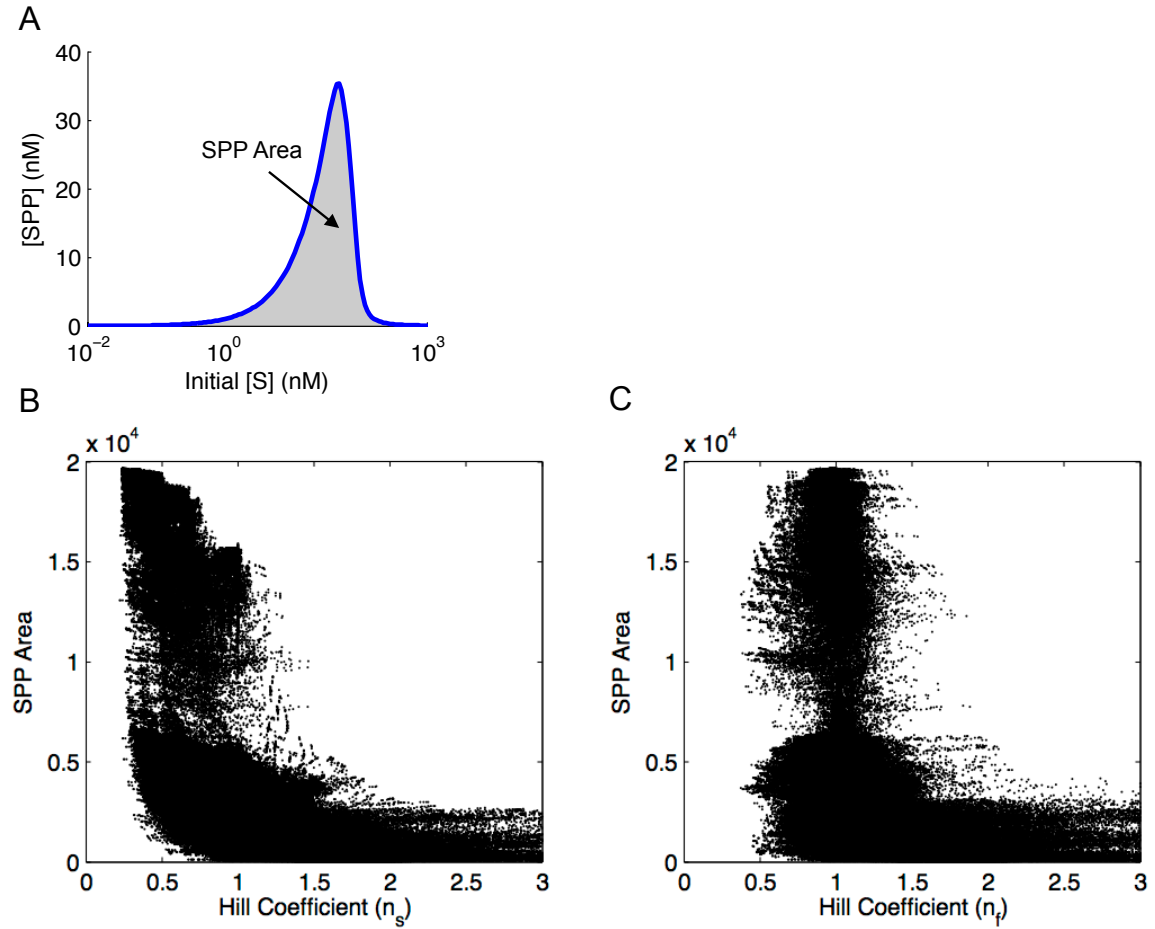

Figure 4. Stoichiometrically asymmetric dimer accumulation is a major determinant of cooperativity. (A) An example of how "SPP area" (shaded region) is calculated. (B) Scatterplot showing the correlation between Scatchard Hill coefficients (n_s) and their corresponding SPP areas for each of the 3^{12} (531,441) simulations. The correlation is highly significant ($\rho=-0.48$, $p<0.001$). (C) Scatterplot showing the correlation between functional Hill coefficients (n_f) and their corresponding SPP areas for each of the 3^{12} simulations. The correlation is significant ($\rho=-0.23$, $p<0.001$).
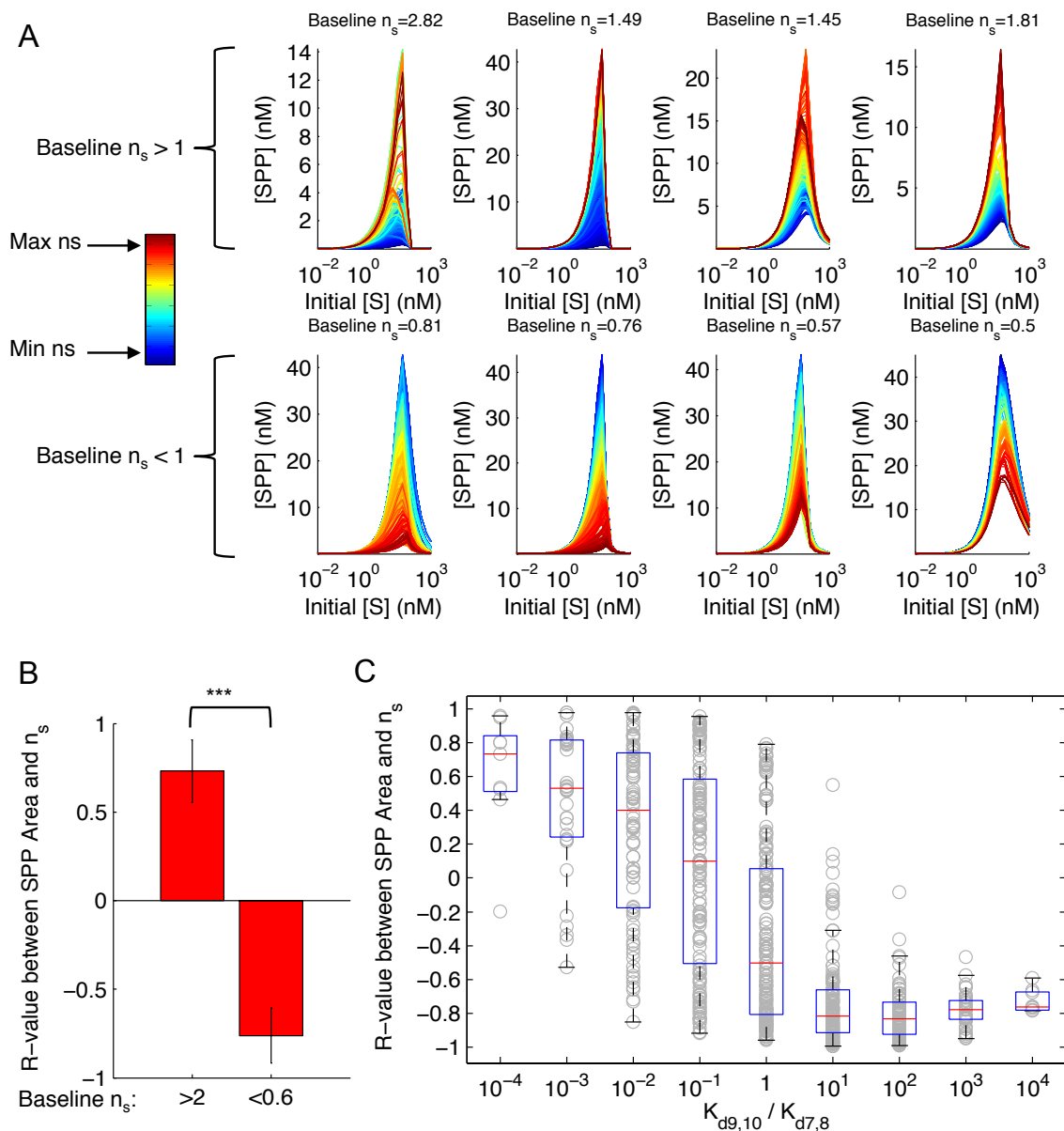
Figure 5. Effect of changes in dimerization affinity on asymmetric dimer accumulation.
(A) Each plot represents one example set, in which dimerization parameters are altered (to be either 0.1, 1, or 10 s^{-1} or $nM^{-1}s^{-1}$) but signal binding parameters are held constant (3^6 total simulations per plot), and individual simulations are colored according to that simulations' Scatchard hill coefficient. Dark red and dark blue represent the maximum and minimum hill coefficient, respectively, for that set. Sets' cooperativity behavior is sometimes positively correlated (top panel) and sometimes negatively correlated (bottom panel) with SPP area. (B) Bar plot showing the mean of the Pearson's r correlation coefficients, which capture the correlation between cooperativity and SPP area, for sets with a baseline greater than 2 (left) or less than 0.6 (right). The two groups are strongly statistically different ($p<10^{-102}$). Error bars depict the standard deviation. (C) Boxplots show the relationship between Pearson's r correlation coefficients and the ratio between the dissociation constants $K_{d9,10}$ and $K_{d7,8}$ $((k_9/k_{10})/(k_7/k_8))$.